acta physica slovaca vol. 45 No. 4, 491 – 498 August 1995

EVANESCENT-WAVE PENETRATION DEPTH IN CAPILLARY OPTICAL FIBRES: CHALLENGES FOR THE LIQUIDS SENSING

R. Brunner, J. Doupovec, F.Suchý, M. Berta
Institute of Physics, Slovak Academy of Sciences, Dúbravská cesta 9, 842 28 Bratislava, Slovakia

Received 4 May 1995, accepted 21 June 1995

A new type of a capillary optical fibre (COF) and its sensoric application is presented for the first time. Attention is focused to the theoretical evaluation of the electromagnetic field distribution across the cross-section of COF and to its preparation. The refractive index of the substance, n_1, introduced in the capillary volume has been taken as a parameter in theoretical and practical analyses. According to the theoretical analyses, the decrease of n_1 shifts the maximum of the evanescent field intensity toward the fibre substrate (cladding). The preform of COF was prepared by means of MCVD and the fibre was pulled without the overpress inside the preform. The core was deposited by SiO_2:GeO_2 ,substrate by SiO_2:P_2O_5. In order to investigate the sensoric properties of COF, the dependence of overall attenuation of COF filled with various liquids with broad range of refractive indices were measured.

1. Introduction

The present theoretical interest in the development of evanescent field fibre optic sensors gives a rise to their new applications [1]. These sensors are mostly based on the measurement of transport properties of so-called sensoric optical fibres, which are modified by means of substances of interest, placed in the vicinity of fibre cores. The most intensive changes of these transport properties take place in the fundamental absorption at the IR frequences. Many problems in the IR detection technique, as well as in the IR waveguides preparation motivate the development of new sensoric fibres and principles. Among these, nowadays the sensors based on the measurement at higher overtones which are well shifted into the near IR or visible range of spectra are of great interest. This technique seems to be very promising for the new practical applications too.

The so called "Evanescent Fibre Spectroscopy" is based on the interaction between the evanescent field of fibre and selectively absorbing medium placed in this field [3]. Contrary to the fibres with liquid cores or hollow optical waveguides where the transmitted energy is absorbed directly inside the core, in the case of evanescent fibre optic sensors the absorption is mainly caused by the medium outside the core and this can be considered the main advantage of this sensors.

The aim of this work was to find out the theoretical dependence of the intensity of the electromagnetic field across the COF and the appropriate penetration depth of the evanescent field into the capillary hole, as well as to its changes caused by different liquids present inside the hole of the COF.

The preparation of the COF and an appropriate sensoric configuration for liquids refractive indices sensing will be also described.

2. Electromagnetic field in COF.

The distribution of electromagnetic field in COF can be found from the scalar wave equation [4]:

$$\frac{\partial^2 R}{\partial r^2} + \frac{1}{r}\frac{\partial R}{\partial r} + (n^2k^2 - \beta^2 - \frac{m^2}{r^2})R = 0 \qquad (1)$$

The tubular core structure was firstly investigated by Barlow in [5]. He showed that the electromagnetic field in such structure rather differs from the field of a weakly guiding cylindrical waveguide. A more detailed study was performed by Berta [6].

Now we present an alternative approximative solution of this problem based on the properties of the asymptotic expression of the Bessel functions. The presented approach utilises the properties of the tubular core structure and the results are also valid for COF (as a special case of tubular core fibres).

Three homogeneous domains can be distinguished in the cross-section of the idealised tubular waveguide. The central part of the waveguide is composed from the material with the refractive index n_1, the second layer is the core of the waveguide with the refractive index n_2, and the third layer is cladding with the refractive index n_3. Therefore:

$$\begin{aligned} n(r) &= n_1 \quad \text{for} \quad r < a_1 \\ n(r) &= n_2 \quad \text{for} \quad a_1 < r < a2 \\ n(r) &= n_3 \quad \text{for} \quad r > a_2 \end{aligned} \qquad (2)$$

Relations $n_1 < n_2, n_3 < n_2$ hold simultaneously.

The tubular waveguide is characterised by Equ. (2), where $\beta > k.n_1$ is the propagation constant of the tubular waveguide. The hollow fibre (i.e. fibre with cavity in domain 1) is the COF. Our following computations are valid for both types of waveguide.

We suppose that condition $\beta > k.n_1$ is satisfied for each mode in the investigated waveguide. The inequality $n_1 < n_3$ meets this condition. As a result of this, only the evanescent wave spreads in domain 1. Since the mode field is localised in the core, condition $\beta > k.n_3$ must be satisfied. Moreover, $\beta \leq k.n_2$ is valid for each waveguide. Due to these restrictions, the solution of the scalar wave equation R_1, R_2, R_3 for the domains 1, 2, and 3, respectively, can be expected in the form:

$$R_1 = \sqrt{2\pi}\, A_1\, I_m(\frac{W_1\, r}{a_1}), \quad W_1 = a_1\sqrt{\beta^2 - k^2n_1^2} \quad \text{for } r \leq a_1 \qquad (3)$$

$$R_2 = \sqrt{\frac{\pi}{2}}[\cos\mu\, J_m(\frac{U_2\, r}{a_2}) + \sin\mu\, Y_m(\frac{U_2\, r}{a_2})],$$

$$U_2 = a_2\sqrt{k^2n_2^2 - \beta^2} \qquad \text{for } a_1 \leq r \leq a_2 \qquad (4)$$

$$R_3 = \sqrt{\frac{\pi}{2}}\, A_3\, K_m(\frac{W_3\, r}{a_2}), \quad W_3 = a_2\sqrt{\beta^2 - k^2n_3^2} \quad \text{for } r \geq a_2 \qquad (5)$$

where the constants A_1, A_3, and μ obey the continuity conditions of tangential components of the field on the boundaries 1-2 and 2-3.

The energy transmitted by the mode is localised mostly in the core of the waveguide and in its closest neighbourhood. Only the evanescent wave spreads out of core. Since its amplitude decreases rapidly with increasing the distance from the core, we may restrict our analysis to the domain around the core (layer 2).

The arguments of the Bessel functions reach the highest values in this domain, especially if a_1/a_2 tends to 1. The asymptotic expansion of the Bessel functions can be introduced in this case. If we restrict the expansion to the first term, we obtain from (3), (4), and (5) [7]:

$$R_1 \approx A_1\sqrt{\frac{a_1}{W_1}}\,\frac{1}{\sqrt{r}}\exp(\frac{W_1 r}{a_1}) \qquad (6)$$

$$R_2 \approx \sqrt{\frac{a_2}{U_2}}\,\frac{1}{\sqrt{r}}\cos[\frac{U_2 r}{a_2} - \mu - (m + \frac{1}{2})\frac{\pi}{2}] \qquad (7)$$

$$R_3 \approx A_3\sqrt{\frac{a_2}{W_3}}\,\frac{1}{\sqrt{r}}\exp(-\frac{W_3 r}{a_2}) \qquad (8)$$

Substituting R_1, R_2, and R_3 into the boundary conditions, the unknown parameters A_1 and A_3 may be excluded. As a result we obtain two equations:

$$\frac{W_1}{U_2 d} = -\tan[U_2 d - \mu - (m + \frac{1}{2})\frac{\pi}{2}] \qquad (9)$$

$$\frac{W_3}{U_2} = \tan[U_2 d - \mu - (m + \frac{1}{2})\frac{\pi}{2}]$$

where $d = a_1/a_2$. The equations contain two unknown parameters μ and β, where β is included in W_1, W_3, and U_2.

Parameters m and μ can be found in the same term $\mu - (m + \frac{1}{2})\frac{\pi}{2}$ in equations (9) and they can be excluded together from (9). Therefore, the modal phase constant β is independent of the azimuthal mode number m and the modes with different m show the same β. This leads to the next mode degeneration, where the modes are completely independent of the azimuthal mode number m. This degeneration occurs as a result of used approximations (6),(7), and (8).

After the substitution $\mu^* = \mu + (m + \frac{1}{2})\frac{\pi}{2}$, equations (9) takes the form:

$$\mu^* = U_2 d + \arctan\frac{W_1}{U_2 d} + i_1\pi \qquad (10)$$

$$\mu^* = U_2 - \arctan\frac{W_3}{U_2} + i_3\pi \qquad (11)$$

where i_1 and i_3 are integers. The presence of these integers is a result of periodicity of the function tangens. Arctg means the main value of function arcus tangens. After eliminating μ^* we obtain

$$U_2(1-d) = \arctan\frac{W_1}{U_2 d} + \arctan\frac{W_3}{U_2} + i\pi \qquad (12)$$

where $i = i_1 - i_3$. After substitutions: $x_1 = k(a_2 - a_1)\sqrt{n_2^2 - n_1^2}$, $x_3 = k(a_2 - a_1) \times \sqrt{n_2^2 - n_3^2}$, $x(i) = k(a_2 - a_1)\sqrt{n_2^2 - (\beta(i)/k)^2} = k(a_2 - a_1)\sqrt{n_2^2 - n_{ef}^2(i)}$, where n_{ef} is the effective refraction index, we obtain Equ.(12) as a transcendental equation for $x(i)$:

$$x(i) = \arccos\frac{x(i)}{x_1} + \arccos\frac{x(i)}{x_3} + i\pi \qquad (13)$$

Modal phase constants can be expressed as $\beta(i) = k.n_{ef}(i)$. We describe the field of the COF using the dispersion relation B(V,i). I.e., we have to find the dependence of the normalised phase parameter B on the normalised frequency V. The parameter of the i-th mode B(V,i) [abbreviated as B(i)] has been defined as:

$$B(i) = \frac{n_{ef}^2(i) - n_3^2}{n_2^2 - n_3^2}. \qquad (14)$$

The shape of the electromagnetic field in 1, 2, and 3 can be found from R_1, R_2, and R_3. Because parameter $\beta(i)$ has been known (see (13)), we can estimate the unknown values A_1, A_3, and μ^* . A_1 can be calculated using the condition $R_1(a_1) = R_2(a_1)$, where μ is expressed from (10). We obtain

$$A_1 = (-1)^{i_1}\sqrt{\frac{W_1}{U_2 d}}\exp(-W_1)\cos(\arctan\frac{W_1 d}{U_2}). \qquad (15)$$

Similarly, A_3 is calculated using the condition $R_2(a_2) = R_3(a_2)$, and μ is expressed from (11):

$$A_3 = (-1)^{i_3}\sqrt{\frac{W_3}{U_2}}\exp(W_3)\cos(\arctan\frac{W_3}{U_2}) \qquad (16)$$

It can be shown that the values i_1 and i_3 may be chosen as arbitrary. However, in order to obey boundary conditions the relation $i = i_1 - i_3$ must be hold. We may put $i_1 = $ i, $i_3 = 0$.

We have obtained the approximative functions describing the electromagnetic field in the COF. The axial components of electric and magnetic vector can be expressed as ([4]):

In domain 1:

$$E_z \approx \sqrt{\frac{a_2}{U_2}}\cos(\arctan\frac{W_1}{U_2 d})\frac{1}{\sqrt{r}}\exp(W_1(\frac{r}{a_1} - 1))\cos(m\varphi)\exp(-j\beta\ z) \qquad (17)$$

$$H_z \approx \sqrt{\frac{a_2}{U_2}}\cos(\arctan\frac{W_1}{U_2 d})\frac{1}{\sqrt{r}}\exp(W_1(\frac{r}{a_1} - 1))\sin(m\varphi)\exp(-j\beta\ z) \qquad (18)$$

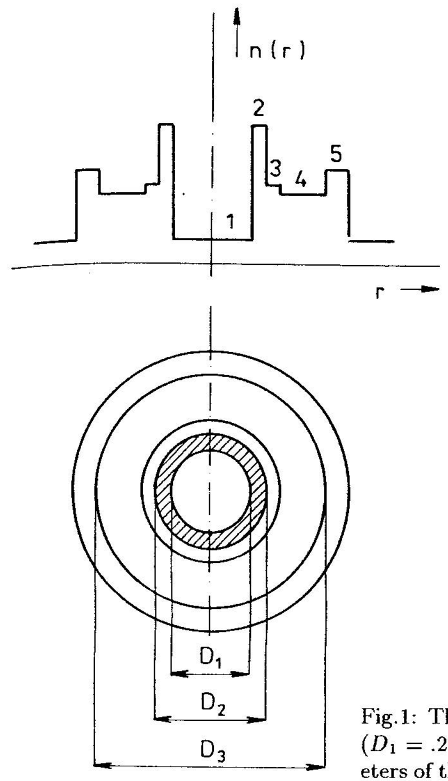

Fig.1: The schematic refractive index profile of the COF ($D_1 = .205mm$, $D_2 = 0.211mm$, $D_3 = 0.3mm$,are diameters of the hole, core and fiber, resp.,$n_2 - n_3 = 10.10^{-3}$.)

In domain 2:

$$E_z = \sqrt{\frac{a_2}{U_2}}\frac{1}{\sqrt{r}}cos(\frac{U_2 r}{a_2} - \mu^*)\cos(m\varphi)\exp(-j\beta\ z) \qquad (19)$$

$$H_z = \sqrt{\frac{a_2}{U_2}}\frac{1}{\sqrt{r}}cos(\frac{U_2 r}{a_2} - \mu^*)\sin(m\varphi)\exp(-j\beta\ z) \qquad (20)$$

In domain 3:

$$E_z = (-1)^i\sqrt{\frac{a_2}{U_2}}\cos(\arctan\frac{W_3}{U_2})\frac{1}{\sqrt{r}}\exp(W_3(1 - \frac{r}{a_2}))\cos(m\varphi)exp(-j\beta\ z) \qquad (21)$$

$$H_z = (-1)^i\sqrt{\frac{a_2}{U_2}}\cos(\arctan\frac{W_3}{U_2})\frac{1}{\sqrt{r}}\exp(W_3(1 - \frac{r}{a_2}))\sin(m\varphi)exp(-j\beta\ z) \qquad (22)$$

Radial and azimuthal components of the field can be calculated using these axial components ([4]).

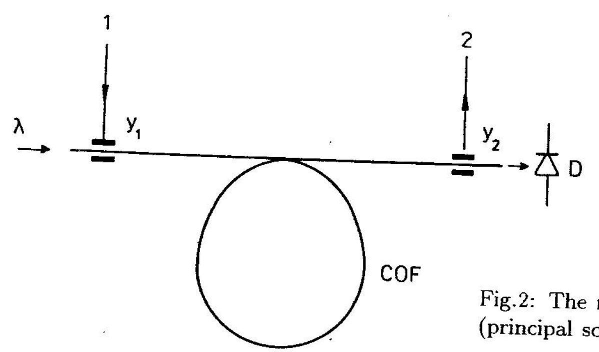

Fig.2: The measurement of COF attenuation (principal schema)

Table 1.

Sample No.	c wt %	n1	I(rel) (800 nm)	Fiber type	W1	R [%]
1	0	1.4622	0.000	Liq. core	32.25	4.00
2	2	1.4588	0.000	capillary	62.28	1.93
3	5	1.4578	0.000	capillary	69.46	1.65
4	10	1.4558	0.000	capillary	82.43	1.22
5	20	1.4398	0.003	capillary	154.53	0.36
6	50	1.4083	0.152	capillary	242.00	0.12
7	75	1.3813	0.417	capillary	296.69	0.07
8	100	1.3588	0.930	capillary	334.99	0.05

3. Preparation of COF

The preparation of the preform for this fibre was performed via the MCVD process [8]. The core was deposited by the SiO_2:GeO_2 and the cladding by SiO_2:P_2O_5. Schematically, the refractive index profile is depicted on the Fig. 1.

The pulling of the fibre from the deposited tube was performed without the overpress inside the tube preform. The pulling temperature was $2050°C$, pulling speed 0.2 m/s. The UV cured epoxy-acrylate was used as a primary buffer.

4. Attempt for sensoric application of COF

In order to verify the the influence of theoretically predicted evanescent-field penetration depth on the transmission properties of the COF a simple experiment was realised. The principle scheme of the set-up which we used is shown in the Fig. 2.

The chopped monochromatic light with spectral width about 5 nm is coupled into the collapsed end of the COF. Simultaneously with the light the gas or liquid substances are introduced into the capillary through the small openings in the COF. This originally developed Y liquids[gas]-light branch-lines by such a means permits to refill the COF with decirable liquids or gases, and simultaneously to measure their optical guiding

properties. The output end of this COF, where the Y coupler was also used, is coupled to the photodetector D. The standard lock-in detection scheme was used in the experiment as well.

The COF which we used had the length of 5 meters and other parameters according to the Fig.1. In order to suppress the bending-induced effects, the coil of the COF had a diameter of 0.25 m. The liquids were flushed through the COF by means of a small argon overpress without the need to break the optical coupling.

Table I gives the calculated and measured values of the COF. Geometrical and optical waveguide parameters are shown in Fig. 1. The hole of the COF was filled with mixture of ethylalcohole and toluene in order to vary the refractive index n_1. The concentration c is given in weight percents of contents of ethylalcohol in toluene. Refractive index n_1 of liquid mixtures was measured by Abbe refractometer at $20°C$ by spectral D-line. The measured light intensity I(rel) is given as a ratio of signals for full and empty COF respectively, at wavelength 800 nm. Optical signal was registered by Ge photodetector (see Fig. 2, item D). W_1 is the calculated decay parameter, which represents the penetration depth (see Eqs. 17, 18). Value R is the ratio (in per cents) of the mode pover in cavity vs. total mode power calculated according to Eqs. (17) - (22). The compatibility between this theoretically calculated depth and experimentally observed attenuation is evident. Moreover, by using this toluene - ethylalcohol mixture it was possible to observe two other light guiding states of this filled COF, which depend on the absolute value of n_1 :

[1.] state, where $n_1 > n_2$, and well known liquid-core optical fiber occur,

[2.] state, where n_1 is near the same as n_2, and the situation like the "weekly guiding fibers" take place.

In the first case, the light is guided through this liquid core, and therefore this process is preferentially influenced by its purity and absorption. The measured attenuation reflects this fact. In the second case the coupling of the guided modes between the liquid core and solid core occurs. New geometrical and optical guiding conditions arise, which influenced the transport properties of this fiber.

4. Conclusion

The depth of the electromagnetic field penetration into the volume of the COF as well as the electromagnetic field distribution in its core and cladding has been calculated. The depth of the evanescent field penetration depends on the value of the refractive index of substance introduced inside the COF. The analyses has shown that the increase of n_1 causes the enhancement of the evanescent field in the substance. This new type of optical fibre and its preform was prepared by the MCVD process and by the standard drawing technique. In order to apply the COF as a sensor of the refractive index variations we have realised the original Y coupler providing the coupling of light into the first branch and the measured substance into second one. Experimentally, we have investigated the influence of refractive index variations of the liquid introduced inside the COF on its transmission properties. The measured values coincide well with the calculated values of evanescent field penetration depths.

Acknowledgement The authors would like to acknowledge to S. Husek, V. Zapala and O. Obrovac for their assistance in the experimental part of this work and Copernicus project No. CIPA-CT94-0140 for the financial support.

References

[1] J. Dakin, B.Cushaw: *Optical Fibre Sensors: Principles and Components* Artech House Inc., USA 1988.

[2] M. Saito, S. Sato, M. Miyagi: in *Chemical, Biochemical and Environmental Fiber Sensors IV.* Proc. SPIE, Boston 1992 (ed. Robert A. Lieberman).

[3] B.D. Mac Craith, V. Ruddy, S. McCabe: in *Chemical, Biochemical and Environmental Fiber Sensors III.* Proc. SPIE, Boston 1991 (Ed. Robert A. Lieberman). Published by SPIE, Vol. 1587, p. 310.

[4] D. Marcuse: *Light Transmission Optics.* Princeton, New Jersey, Van Nostrand Reinhold 1972.

[5] H. M. Barlow: *J. Phys. D: Appl. Phys.* **16** (1983) 1439;

[6] M. Berta: *Study of critical frequency of monomode optical fibre waveguides.* PhD Thesis, Bratislava 1993.

[7] F. W. J. Olver: *Asymptotic and special functions.* New York and London, Academic Press 1974.